Laser ablation of a triazene polymer studied by ns-interferometry and shadowgraphy

M. Hauer[a], D.J. Funk[b], T. Lippert[a*], A. Wokaun[a]
[1] General Energy Research, Paul Scherrer Institut, 5232 Villigen PSI, Switzerland
[2] DX-2, MS C920, Los Alamos National Laboratory, Los Alamos, NM 87545

ABSTRACT

Nanosecond-interferometry and shadowgraphy is used to observe the dynamic behavior of the etching process during and after the irradiation pulse. Commercially available polymers exhibit quite often poor laser ablation properties for irradiation wavelengths ≥ 248 nm. At these wavelengths the absorption is due to the quite photostable aromatic groups. A photolabile triazene polymer was selected to compare the influence of a photolabile group on the laser ablation process. The photochemical active triazene reveals a strong absorption band at 332 nm and is responsible for the observed high etch rates and the low threshold for 308 nm irradiation. The absorption coefficients at 193 nm and at 308 nm are comparable, allowing to study the influence of the different absorption sites by ns-interferometry and shadowgraphy measurements. The etching of the triazene polymer starts and ends with the laser beam. No surface swelling, which is assigned to photothermal ablation, is detected for fluences above the threshold of the ablation. The expansion of the laser ablation induced shockwave was measured for the photolabile triazene polymer and the photostable polyimide. The speed of the shockwave increases with fluence and is higher for irradiation with 193 nm than for 308 nm. A shockwave with equal or higher velocity is observed for the triazene polymer than for the polyimide.

Keywords: laser ablation, shadowgraphy, interference surface profiling, interferometry, triazene polymer, photopolymer

1. INTRODUCTION

Laser ablation of polymers was first reported in 1982[1,2], but the ablation mechanism remains still controversial. It has been emphasized that a better understanding of the time scale of the ablation process is fundamental for an understanding of the physical chemistry of this phenomenon. Many different approaches, such as time resolved absorption[3] and emission spectroscopy[4],time resolved Raman spectroscopy[5,6], time resolved infrared spectroscopy[7,8] and time resolved quadrupole mass spectroscopy[9-12] were used to obtain a better understanding of the ablation process.

Ns-surface interference measurements have shown that time resolved surface profiling of the ablated area can give valuable information about the ablation process. It has been demonstrated that some polymers exhibit a pronounced swelling before ablation of the surface is observed[13,14], whereas the ablation process of an other polymer starts and ends with the laser pulse[15]. The surface swelling was attributed to a photothermal process, while the absence of this swelling was interpreted as indication for a photochemical process.

In this study the laser ablation process of a photolabile triazene polymer, which exhibits superior laser ablation characteristics (sharp ablation edges, no debris, low threshold fluence and high etch rates at low fluences) is studied by using ns-interferometry. The polymer exhibits an absorption maximum around 200 nm. This absorption is due to the photostable aromatic system. A second absorption maximum around 332 nm is due to the photolabile triazene group. Both absorption maxima have similar absorption coefficients. The influence of the different chromophores on the changes of surface morphology during the ablation process can be studied by irradiating at 308 nm and 193 nm.

Complementary information can be obtained by shadowgraphy, where the laser ablation induced shockwave is analyzed. It has been shown, that the ejection of solid material can be detected by these measurements[3,13,16] and that in some cases the expansion of the shockwave cannot be fully explained by the energy deposited from the laser. In this case it is necessary to include the decomposition enthalpy of the polymer for the shockwave analysis[17]. The

High-Power Laser Ablation IV, Claude R. Phipps, Editor, Proceedings of SPIE Vol. 4760 (2002)

shadowgraphy measurements were also performed with polyimide, to have a reference of a standard polymer with very similar absorption properties.

2. EXPERIMENTAL

The triazene polymer (shown in Figure 1) was prepared by a previously described method[18]. The 1 to 2 µm thick polymer films were spin coated from a chlorobenzene solution (10 % polymer) and dried at 40 °C for 24 h. The polyimide film (75 µm thick, Kapton™ HN) was obtained from DuPont. All measurements were performed under ambient pressure at room temperature.

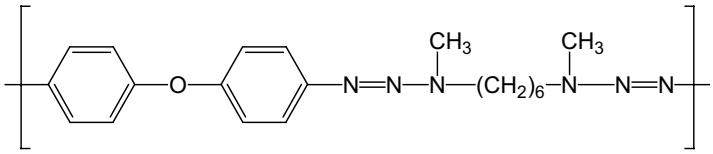

Figure 1: Chemical structure of the triazene polymer

The experimental setup for the surface interference measurements is shown in Fig. 2. For the 308 nm irradiation a Compex 205 XeCl excimer laser from Lambda Physik (FWHM 30 ns) was applied, while for the irradiation at 193 nm a LPX 301i ArF excimer laser (Lambda Physik, FWHM of 25 ns) was used. The probe laser (2nd harmonic of an Brillant Bω Nd:YAG laser from Quantel with a FWHM of 5 ns) was used in Michelson interferometric setup. The probe beam was divided by a beamsplitter (50:50) and one beam is reflected by a wedged substrate (allowing to select the reflection from the air/quartz interface). The other beam passes from the rear side of the sample through the wedged substrate and polymer and is reflected at the polymer/air interface. This has the advantage that the ejected material does not disturb the probe beam. Both beams are recombined in the beamsplitter and create therefore an interference fringe pattern. Changes of the surface or optical density of the polymer will change the effective path length of the probe beam through the polymer (shown in Figure 2), resulting in a fringe shift.

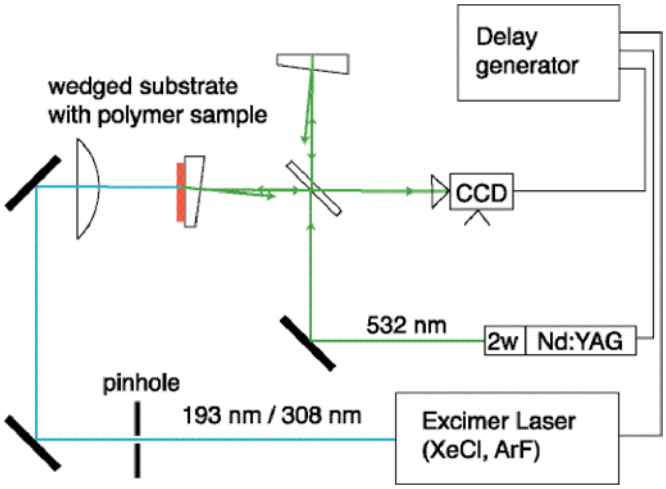

Figure 2: Surface interference setup

The optical density of the polymer was obtained by comparing the final fringe shift with the ablation depth measured with a surface profilometer (Dektak 8000 from Sloan Technologies). The fringe shift is proportional to the surface displacement by assuming that the ablation process does not affect the optical density. Both lasers were timed with a delay generator (DG 535 from SRS) and the surfaces fringes were recorded with a CCD camera. In the following the time t = 0 ns was chosen as the time where the laser pulse reaches 1 % of its maximum intensity. The surface profile at a specific time can be extracted by evaluating (described later) the fringe shifts.

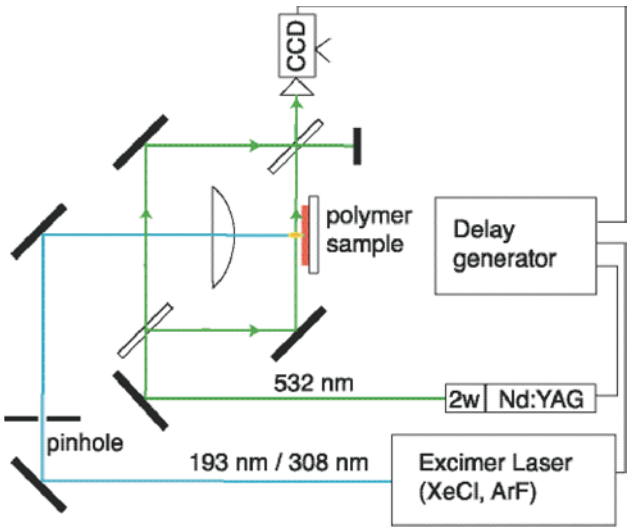

Figure 3: Shadowgraphy setup

For the shadowgraphy experiments the optical pathway of the probe laser was modified to a Mach-Zehnder interferometer setup (shown in Figure 3). One beam of the interferometer passes parallel to surface of the polymer, through the ablation plume, while the other beam is unaffected by the ablation process. Both beams are recombined in a second beamsplitter where the fringe pattern is created. The compressed (i.e. ablation products and air) gases in the shockwave of the ablation have a higher optical density than the ambient atmosphere. A fringe shift results, which is proportional to the changes of the optical density and path length of the probe beam through the ablation plume.

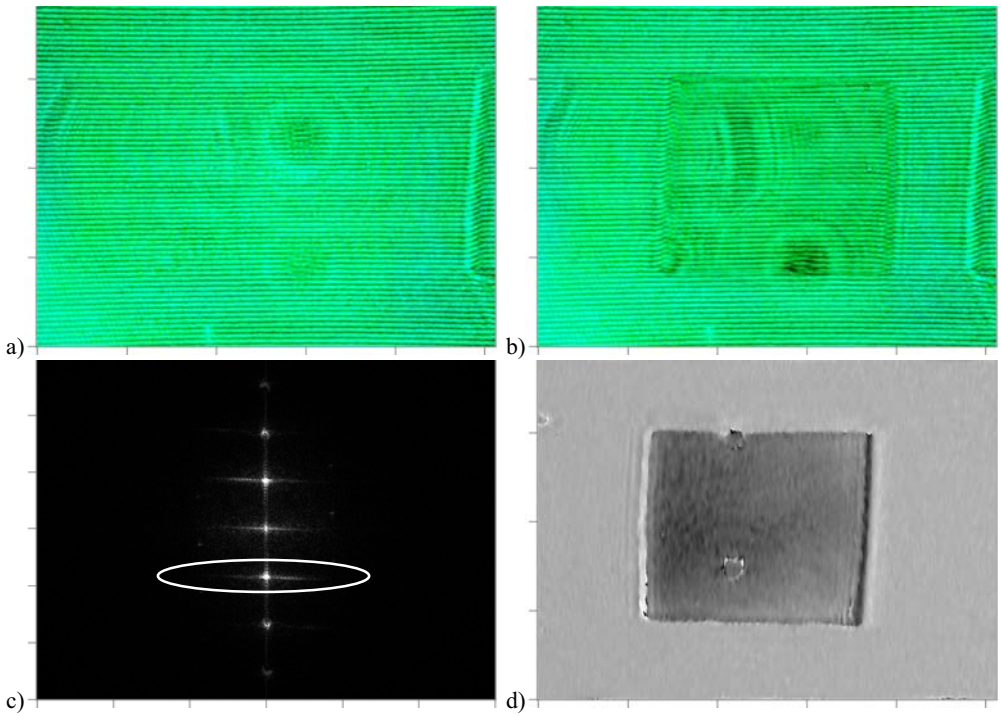

Figure 4: a) Reference picture (surface interference), b) Measurement picture (surface interference),
c) Resulting image after 2D FFT, the region of interest is marked by the white oval
d) Resulting phase shift image

The evaluation of the fringe shifts was done according to a procedure describes earlier[19,20]. Briefly, during both experiments a picture was recorded before (figure 4a) and during/after the pump pulse (figure 4b). These two pictures

were transformed using a 2D fast Fourier procedure (2D FFT). The images can be reduced to the fringe information by selecting one specific peak from the fringes in the 2D FFT images (figure 4c) and filtering all other peaks. The images were then inverse Fourier transformed into the complex space. The phase difference between the reference and the measurement picture is then proportional to the fringe shift (figure 4d). The dynamic range of the phases is limited to 2π. A phase jump will result if the phase shift between both pictures exceeds this limited range. It is very important during the data analysis to include these phase jumps otherwise wrong ablation depths are obtained.

The ablation depth was measured from the phase shift images taken from the surface interference setup. Figure 5 shows a series of images at different delay times. It is obvious, that the phase shift of the non-irradiated area changes from measurement to measurement. This is due to instabilities of the interference pattern, which causes a varying constant offset from measurement to measurement. Therefore the difference between the phase shifts of the irradiated and non-irradiated areas was analyzed. By taking the wavelength of the probe beam, the optical density of the polymer and the phase jumps into the analysis procedure the surface displacement at a specific time during or after the pump laser pulse can be determined.

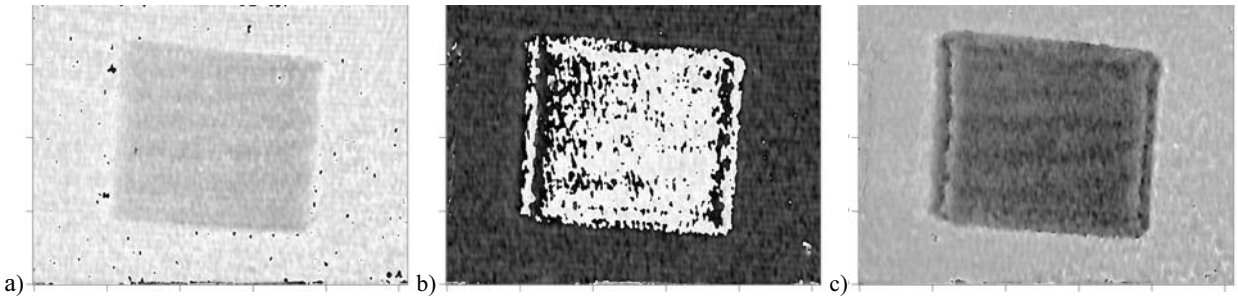

Figure 5: Surface interference phase shift images taken at different delay times. The triazene polymer was irradiated with 210 mJ cm^{-2} at 308 nm. a) 10 ns b) 21 ns c) 31 ns

The shadowgraphy setup was applied to measure the expansion of the shockwave from the phase shift images. Figure 6 shows a series of phase shift images at different time delays. The surface of the polymer is located at the left side of the image. In the area covered by the polymer sample no interference fringes can be seen in the original pictures. The evaluation of the images produces noise in this area (see Figure 6 a,b,c, on the left side) giving the impression of interference patterns. The shockwave of the ablation expands towards the right side of the images. Measuring the distance between the shockwave front and the polymer surface allows to determine the propagation of the shockwave.

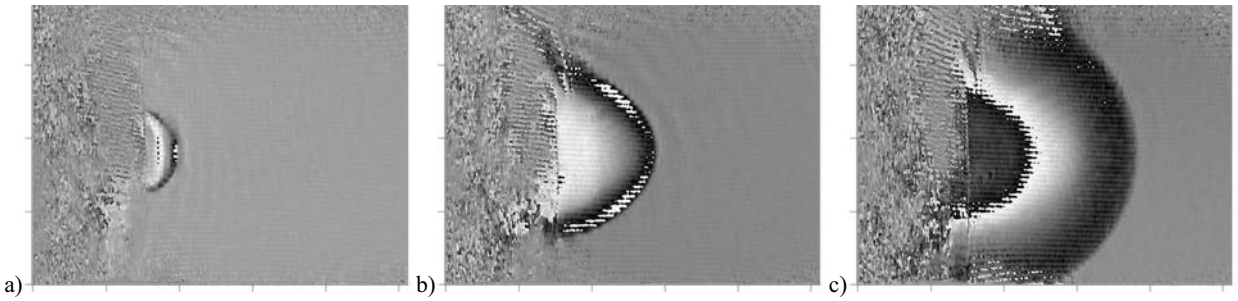

Figure 6: Shadowgraphy phase shift images taken at different delays. The triazene polymer was irradiated with 1050 mJ cm^{-2} at 193 nm a) 120ns b) 710 ns c) 2270 ns

3. RESULTS AND DISCUSSION

3.1 NS-SURFACE INTERFERENCE

The surface displacement of the triazene polymer after irradiation at 308 nm at different fluences is shown in figure 7. The data taken at 10 mJ cm^{-2}, which is below the ablation threshold of the triazene polymer (F_{th}=25 mJ cm^{-2} at 308 nm, measured with multiple laser pulses) reveal a slight surface swelling which starts with the laser pulse and disappears after several seconds. No permanent modification of the polymer surface is observed.

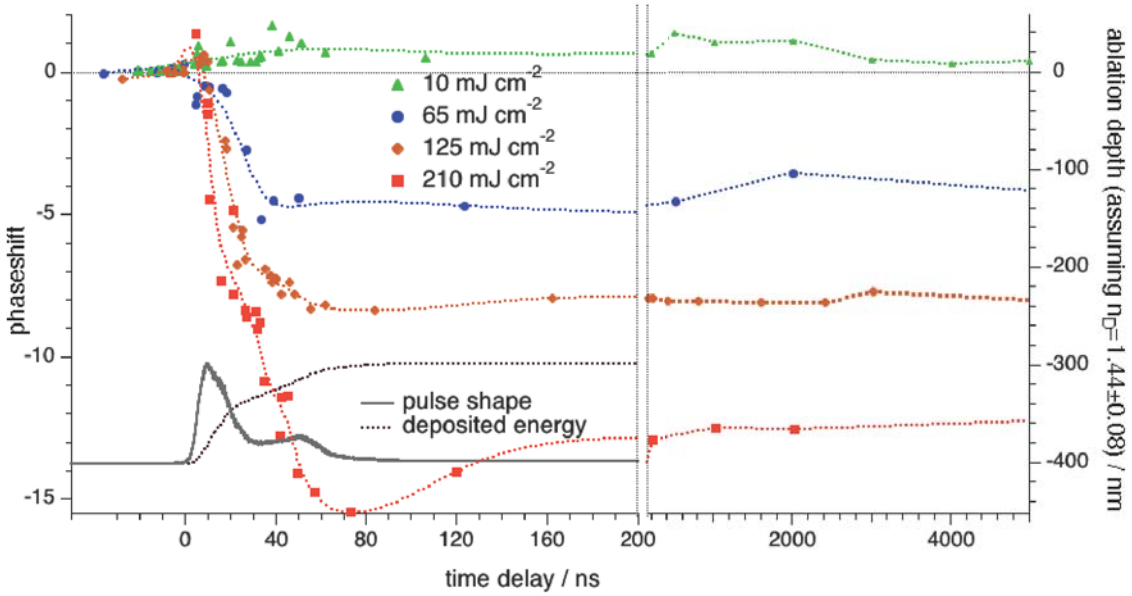

Figure 7: Ablation depth of the triazene polymer after irradiation at 308 nm. A smoothed spline curve is added to guide the eyes along the data points. In the lower left area the relative intensity and integrated power of the laser pulse is included.

At higher fluences the phase shift starts with the laser pulse. At 125 and 210 mJ cm^{-2} a very short positive phase shift is observed. This phase shift may be due to a very dense gas layer, which is created during the initial ablation process. Such a gas layer should have a high optical density, which will cause the reflection of the probe beam at this gas/air interface. When the gas expands the optical density will decrease and the beam will be reflected at the polymer/air interface. Then the decrease of the phase shift corresponds to the ablation of the polymer in the irradiated area. The ablation process ends with laser pulse.

For 65 and 125 mJ cm^{-2} irradiation only minor changes of the ablation depths are observed after the laser pulse. After irradiation with 210 mJ cm^{-2} the ablation continues for about 80 ns. Whether this is an additional effect which only appears at high fluences or large ablation rates is not clear at the moment.

The surface displacement after irradiation at 193 nm is shown in figure 8. The lowest applied fluence is just slightly below the ablation threshold of 12 mJ cm^{-2}. With the start of the laser pulse a very weak phase shift is observed. This phase shift corresponds to an ablation depth of 20 nm. The phase shift remains constant during the first 5 μs but changes to a phase shift corresponding to an ablation depth of about 2 nm after several seconds. Slight changes of the optical density of the remaining polymer by the irradiation may cause this transient phase shift. The examination in an optical microscope revealed no visible changes of the surface.

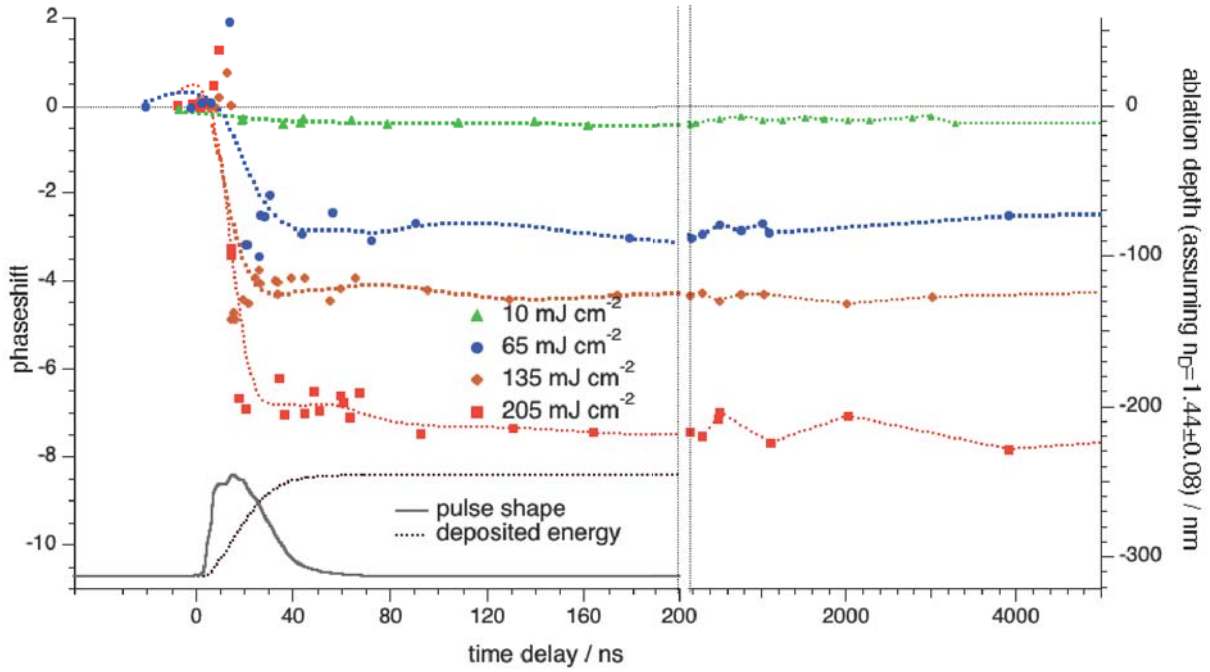

Figure 8: Ablation depth of the triazene polymer after irradiation at 193 nm. A smoothed spline curve is added to guide the eyes along the data points. In the lower left area the relative intensity and integrated power of the laser pulse is included.

All higher fluences reveal a clear ablation of the polymer. The phase shift starts with the laser pulse and an initial fast positive phase shift is observed. This phase shift is attributed to a dense gas layer, as described above. This swelling is more pronounced for 193 nm irradiation than for 308 nm ablation, although the ablation volume for 193 nm is smaller than for 308 nm. The 193 nm photons have higher energies and are absorbed by more chromophores than the 308 nm photons. This results in more gaseous fragments, which can cause a more pronounced dense gas layer. The phase shift decreases very fast after this initial positive phase shift. This decrease is attributed to the ablation of the polymer. After the laser pulse no further surface displacements is observed and the ablation depth remains constant. The final ablations depths are approximately 20 % deeper than the values measured with other methods. This is most probably due to an inhomogeneous beam profile. The ablation depth and the phase shift were measured in the center of the phase shift image. In this area the beam intensity was higher than the average, which was measured across the complete pulse.

The ablation process starts and ends at both wavelengths with the laser pulse. A positive phase shift can only be observed for a very short time (≈ 10 ns). This cannot be explained by a thermal swelling of the polymer surface as observed for other polymers on a much longer time scale[8]. The absence of the thermal swelling and the end of the ablation process with the end of the laser pulse are strong indications, that at both wavelengths a photochemical ablation mechanism is at least partly responsible for the ablation process. The initial ablation speeds are the same for 193 nm and for 308 nm irradiation (see Table 1). For 308 nm the laser pulse is longer, which results in a higher ablation rate.

Table 1: Summary of the initial ablation speed

Fluence mJ cm^{-2}	308 nm	193 nm
210	11 nm ns^{-1}	11 nm ns^{-1}
130	8 nm ns^{-1}	8 nm ns^{-1}
65	4 nm ns^{-1}	3 nm ns^{-1}

3.2 SHADOWGRAPHY

The shockwave first starts with a planar expansion (shown in figure 6a). This expansion changes to a stretched hemisphericaly expansion (the expansion perpendicular to the surface is faster than parallel to the surface, see figure 6b). Only the expansion perpendicular to the surface in analyzed in more detail below.

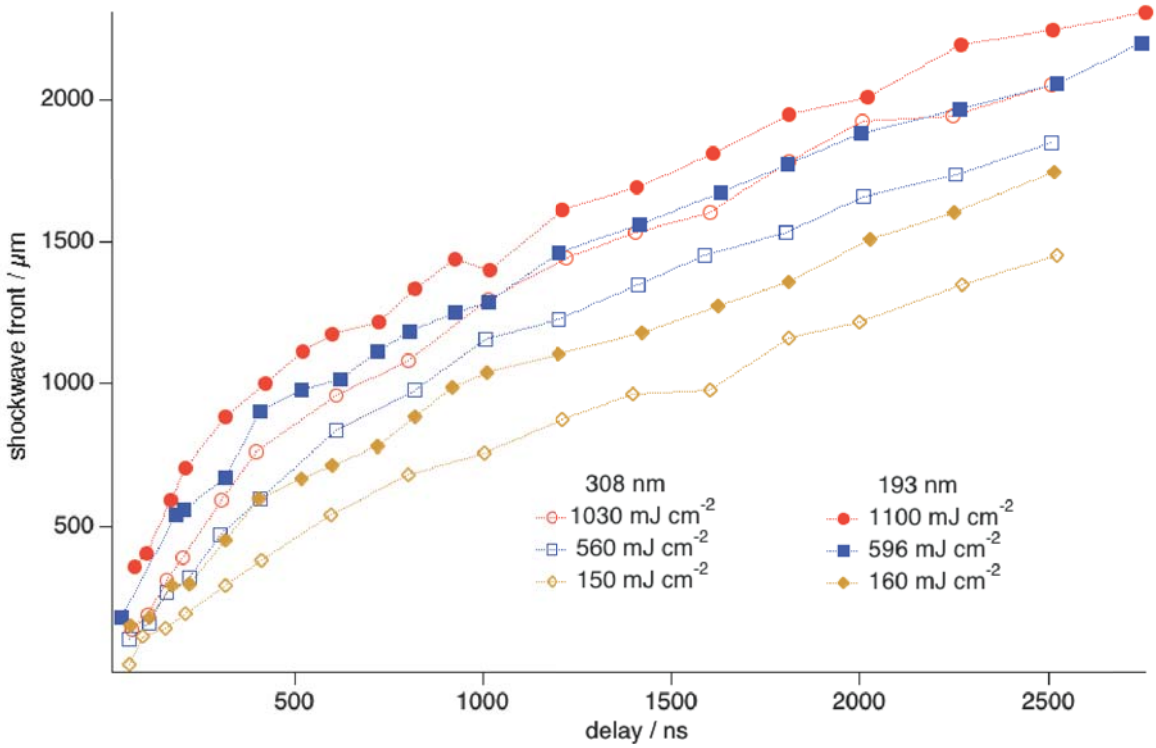

Figure 9: The propagation of the shockwave for variable fluences after irradiation at 193 nm and 308 nm (triazene polymer). (Measured perpendicular to the polymer surface)

The propagation of the shockwave is at all applied fluences faster for irradiation with 193 nm light than for 308 nm (shown in figure 9). At 308 nm the triazene group of the polymer absorbs the laser light. The photon energy at this wavelength is quite low (4.02 eV), resulting mainly in the decomposition of the triazene group. This will result in large molecule fragments. The 193 nm photons are absorbed by the aromatic system in the triazene polymer. These photons have a higher energy (6.59 eV) and are therefore able to break most bonds in the polymer (including the C=C bonds of the aromatic system). This results in more and smaller gaseous fragments than for 308 nm irradiation. TOF-MS analysis has shown, that fragments with masses up to 168 amu are produced during ablation)

Table 2: Chemical properties and ablation parameters of the polymers

	Triazene Polymer		Polyimide	
	193 nm	308 nm	193 nm	308 nm
α_{lin} (cm^{-1})	118.000	100.000	340.000[1]	95.000[2]
α^{eff} (cm^{-1})	214.000	50.000		83.000[2]
F_{th} (mJ cm^{-2})	12	25		60[2]
d (nm pulse-1) at 150 mJ cm^{-2}	118	358	65[3]	78[3]
600 mJ cm^{-2}	183	635	130[3]	353[3]
1000 mJ cm^{-2}	207	737	155[3]	564[3]

[1] from Lit. [21], [2] from Lit. [22], [3] from Lit. [23]

Further indications for this increased fragmentation are the higher effective absorption coefficient, α_{eff}, and the lower ablation rates (see Table 2). This higher α_{eff} for 193 nm irradiation suggests that the energy is deposited in a thinner layer, probably also resulting in smaller fragments. At 308 nm irradiation more polymer is ablated but the extended fragmentation for 193 nm irradiation produces a higher initial velocity of the shockwave

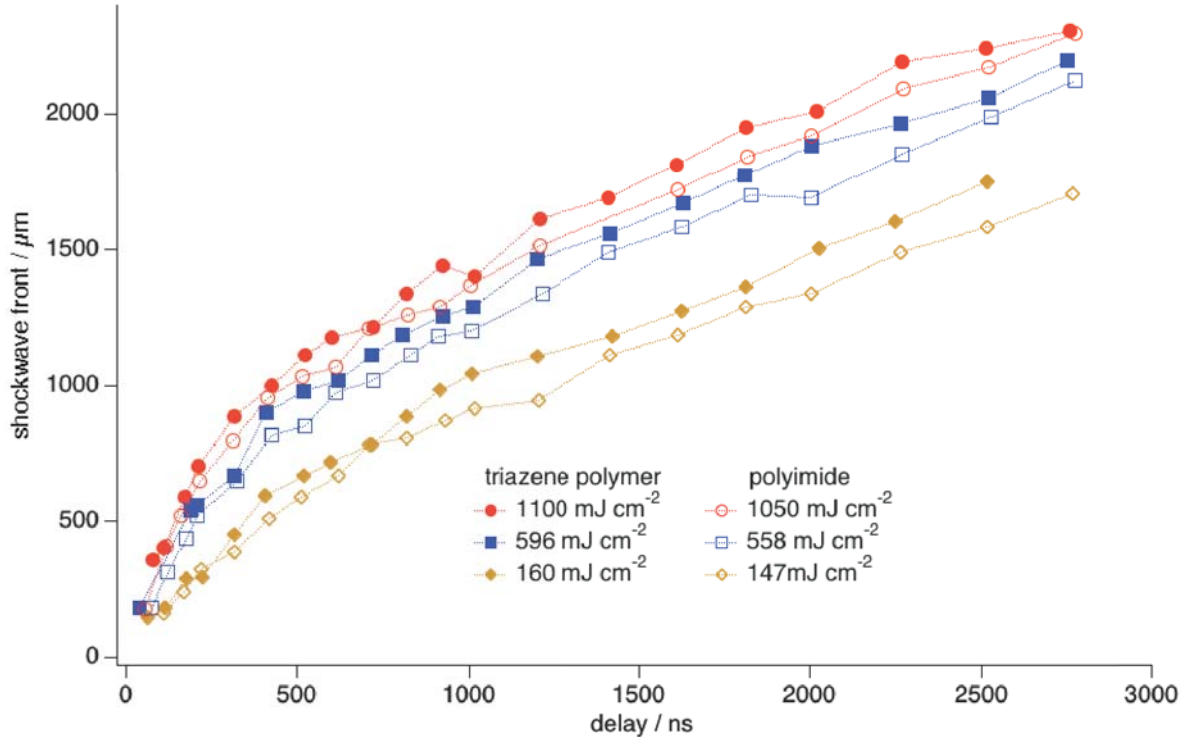

Figure 10: The propagation of the shockwave after irradiation of the triazene polymer at 193 nm for variable fluences (measured perpendicular to the surface of the polymer). Polyimide was included as a reference polymer to quantify the influence of the polymer properties on the ablation process, respectively shockwave propagation.

Figure 10 shows the propagation of the shockwave after 193 nm irradiation of the triazene polymer and polyimide. The velocities of shockwaves from the triazene polymer are always faster than those observed for the polyimide. This is due to the higher activity of the triazene polymer in the ablation process. The higher activity results in higher ablation rates (see Table 2) and a pronounced fragmentation during the ablation process. The higher ablation rates and the further fragmentation will increase the amount of gaseous ablated products (and the pressure in the shock wave) and the shockwave of the triazene polymer will travel at a higher velocity.

Figure 11 shows the propagation of the shockwave of the triazene polymer and polyimide after irradiation at 308 nm. The shockwaves of both polymers move with the same speed at the two higher fluences. Around 400 mJ cm^{-2} the initial velocity of shockwave of the triazene polymer is slightly higher then those observed for the polyimide. This difference becomes even more pronounced at lowest fluence.

At the lower fluences the ablation rates are more dependent on the structure of the polymer than at higher fluences. This becomes obvious when ablation rates of the triazene polymer and the polyimide are compared. (Table 1, at 1 J cm^{-2} $d_{triazene}$ / $d_{polyimide}$ = 1.3 vs. after for 150 mJ cm^{-2} $d_{triazene}$ / $d_{polyimide}$ = 4.5). The large difference in the ablation depths, results in a difference in the amount of gaseous products. Increasing amounts of gaseous products will increase the speed of the shockwave. The initial speed of the shockwaves at higher fluences are similar for 308 nm irradiation, suggesting that the fragmentation is comparable in these measurements.

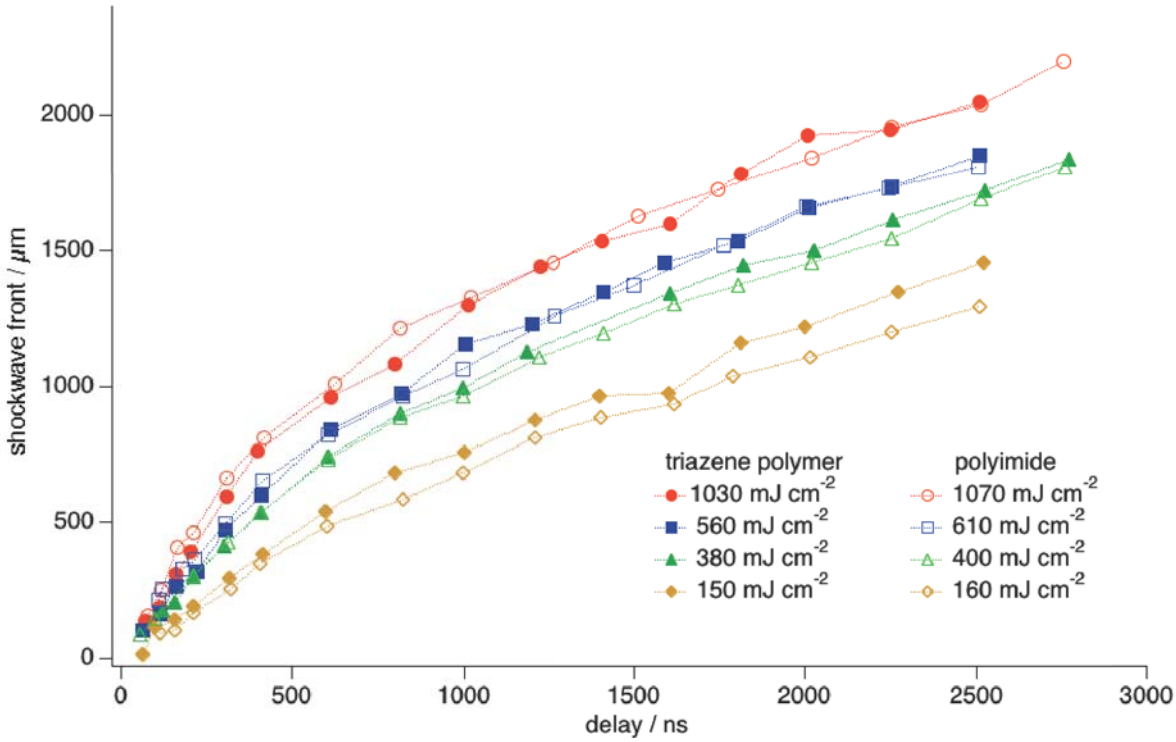

Figure 11: The propagation of the shockwave after irradiation of the triazene polymer at 308 nm for variable fluences (measured perpendicular to the surface of the polymer). Polyimide was included as a reference polymer to quantify the influence of the polymer properties on the ablation process, respectively shockwave propagation.

All initial shockwaves travel with supersonic speeds, i.e. between 970 and 2080 m s^{-1} (Table 3). The initial speed of the shockwave is related to the amount of gases released during the ablation process. Whether this gas is produced by high ablation rates and larger fragments (low fragmentation of the polymer) or by lower ablation rates and smaller fragments (high fragmentation) seems to be of minor importance. The shockwave velocities after 2000 ns are still supersonic and vary between 400 and 500 m s^{-1}. A possible explanation is the volume increase during the expansion of the shockwave. The volume of a hemisphere increases with the cube of the radius. The pressure within the shockwave will decrease at the same time. At some given time the pressure differences, due to different amount of gases, will have only a minor effect on the velocity of the shockwaves. The initial velocities are compiled in Table 3.

Table 3: Summary of the initial shockwave velocities (during the first 500 ns)

	Triazene Polymer		Polyimide	
Fluence mJ cm^{-2}	193 nm	308 nm	193 nm	308 nm
1150	1900 m s^{-1}	1950 m s^{-1}	2100 m s^{-1}	2150 m s^{-1}
580	1850 m s^{-1}	1450 m s^{-1}	1700 m s^{-1}	1400 m s^{-1}
150	1300 m s^{-1}	1000 m s^{-1}	1100 m s^{-1}	900 m s^{-1}

An important error source are the differences in the timing between the different measurements. The averaging period was not constant which effects the measured velocities.

4. CONCLUSION

Ns-interferometry shows, that the ablation process of the triazene polymer starts and ends with the laser pulse. Initially a small positive phase shift is observed. This positive phase shift is transient (10 ns) and followed by a fast negative shift, which is assigned to ablation of the polymer. The positive phase shift is too fast to be assigned to a thermal surface swelling, as observed with other polymers. Therefore the transient phase shift is attributed to dense layer of gaseous ablation products. The ablation initial speeds are the same for 193 nm and 308 nm irradiation. The longer pulse length at 308 nm results in a higher ablation rate.

Shadowgraphy measurements were used to measure the laser ablation induced shockwave for the photolabile triazene polymer and for the polyimide as a photostable reference polymer. The speed of the shockwave increases with laser fluence and is higher for irradiation with 193 nm than for 308 nm. This attributed to the higher energy of the 193 nm photons, which are able to break more bonds than the 308 nm photons and therefore produce a large amount of small fragments. The shockwaves of the triazene polymer ablation reveal an equal or higher velocity than those observed for the polyimide ablation. The triazene polymer is more sensitive to the UV photons (especially at 308 nm) than the polyimide and is ablated with higher efficiencies. The higher ablation rate results in more gaseous products during the ablation process, resulting a faster shockwave.

5. ACKNOWLEDGMENT

This work has been supported by the Swiss National Science Foundation.

6. REFERENCES

[1] R. Srinivasan, V. Mayne-Banton, *Appl. Phys. Lett.* **41**, 576, 1982.
[2] Y. Kawamura, K. Toyoda, S. Namba, *Appl. Phys. Lett.* **40**, 374, 1982.
[3] H. Fukumura, E. Takahashi, H. Masuhara, *J. Phys. Chem. A.* **99**, 750, 1995.
[4] H. Fujiwara, H. Fukumoto, H. Fukumura, H. Masuhara, *Res. Chem. Intermed.* **24**, 879, 1998.
[5] D. E. Hare, D. D. Dlott *Appl. Phys. Lett.* **64**, 715, 1994.
[6] D.E. Hare, J. Franken, D. D. Dlott, *J. Appl. Phys.* **77**, 5950, 1995.
[7] T. Lippert, P. O. Stoutland, *Appl. Surf. Sci.* **109/110**, 43, 1997.
[8] T. Lippert, A. Koskelo, P. Stoutland, *J. Am. Chem. Soc.* **118**, 1551, 1996.
[9] T. Lippert, A. Wokaun, S. C. Langford, J. T. Dickinson, *Appl. Phys. A.* **69**, 655, 1999.
[10] T. Lippert, S.C. Langford, A. Wokaun, G. Savas, J.T. Dickinson, *Appl. Phys. A.* **89**, 7116, 1999.
[11] M. Hauer, J.T. Dickinson, S.C. Langford, T. Lippert, A. Wokaun, *Appl. Surf. Sci.,* in press
[12] D.J. Krajnovich, *J. Phys. Chem. A.* **101**, 1175, 1996.
[13] H. Furutani, H. Fukumura, H. Masuhara, S. Kambara, T. Kitaguchi, H. Tsukada, T. Ozawa, *J. Phys. Chem.* B. **102**, 3395, 1998.
[14] H. Furutani, H. Fukumura, H. Masuhara, *Appl. Phys. Lett.* **65**, 3413, 1994.
[15] H. Furutani, H. Fukumura, H. Masuhara, T. Lippert, A. Yabe, *J. Phys. Chem.* A. **101**, 5742, 1997.
[16] R. Srinivasan, *Appl. Phys. A.* **56**, 417, 1993.
[17] L.S. Bennett, T. Lippert, H. Furutani, H. Fukumura, H. Masuhara, *Appl. Phys. A.* **63**, 327, 1996.
[18] J. Stebani, O. Nuyken, T. Lippert, A. Wokaun, *Makromol. Chem. Rapid Commun.* **206**, 2943, 1993.
[19] M. Takeda, H. Ina, S. Kobayashi, *J. Opt. Soc.* **72**, 156, 1982.
[20] K.T. Gahagan, D.S. Moore, D. J. Funk, J. H. Reho, R.L. Rabie, submitted to *J. Appl. Phys.*, 2002.
[21] S. Küper, J. Brannon, K. Brannon, *App. Phys. A.* **56**, 43 ,1993.
[22] T. Lippert, C. David, J.T. Dickinson, M. Hauer, U. Kogelschatz, S.C. Langford, O. Nuyken, C. Phipps, J. Robert, A. Wokaun*, J. Photochem. Photobiol. A.* **145**, 145, 2001.
[23] R. Srinivasan, B. Braren, R.W. Dreyfus*, J. App. Phys.* **61**, 372, 1987.